Journal of the Korea Academia-Industrial cooperation Society
Vol. 17, No. 12 pp. 98-106, 2016

http://dx.doi.org/10.5762/KAIS.2016.17.12.98
ISSN 1975-4701 / eISSN 2288-4688

Correction of the hardness measurement for pile-up materials with a nano indentation machine

Moon Shik Park

Department of Mechanical Engineering, Hannam University

파일-업 재료에 대한 나노 압입 시험기의 경도 측정값 교정

박문식

한남대학교 기계공학과

Abstract Measurements of the elastic modulus and hardness using a nano indentation machine rely on the equation for the fitted contact area, which is valid for only sink-in materials. For most soft engineering materials that involve pile-up behavior rather than sink-in, the contact area equation underestimates the contact area and thus overestimates the elastic modulus and hardness. This study proposes a correction method to amend erroneous hardness measurements in pile-up situations. The method is a supplemental derivation to the original hardness measurement with the known value of the elastic modulus. The method was examined for soft engineering metals, Al 6061 T6 and C 12200, via tensile tests, nano indentation tests, impression observations, and finite element analysis. The proposed technique shows reasonable agreement with the analytical results accounting for strain gradient plasticity from a previous study.

요 약 본 연구는 공업용 응용이 많은 알루미늄 또는 구리와 같은 재료를 나노 압입 시험기에 의하여 탄성계수 및 경도 값을 얻을 때 파일-업(pile-up) 현상이 생기는 경우 계측 값을 교정할 수 있는 방법에 대해 다룬다. 나노 압입 시험기에 의해 얻어지는 탄성계수와 경도의 측정치는 접촉면적의 피팅(fitting) 식에 의존하게 되는데 이는 오로지 싱크-인(sink-in) 재료에만 유효하다. 그러므로 싱크-인이 아닌 파일-업인 많은 무른 공학재료들에 있어서는 그 접촉면적이 실제보다 적게 계산되고 따라서 탄성계수와 경도는 높게 계산된다. 본 연구에서는 이미 탄성계수를 알고 있는 파일-업 거동을 보이는 재료의 경우에 경도 값을 교정하는 방법을 제안한다. 이 방법을 경금속인 Al 6061 T6와 C 12200에 적용하기 위해 인장시험, 나노 압입시험, 압입자국 측정, 그리고 유한요소해석을 수행하였다. 압입 자국 측정과 유한요소해석을 통하여 두 재료 모두 파일-업 거동이 발생하는 것을 알 수 있었다. 제안한 교정 방법은 싱크-인 접촉면적 값을 파일-업 접촉면적 값으로 늘려 주었고 경도 측정값을 낮추어 주었다. 교정된 경도 값은 별도의 연구에서 다룬 변형률 구배 소성을 고려한 유한요소해석 결과와 잘 일치하였다.

Keywords : Berkovich indenter; Indentation size effect; Hardness measurement; Nano indentation; Pile-up phenomenon;

1. Introduction

Nano and micro indentation tests are becoming popular for the determination of the elastic modulus and hardness of state-of-the-art materials [1-7]. Such tests are attractive because they are nondestructive and eliminate the need for expensive optical impression measurements. Indentation tests are carried out by measuring the load and depth relationship with the harmonic contact stiffness at a resolution of a nanometer, as devised by Oliver and Pharr [8, 9].

Unfortunately, nano and micro indentation results may be erroneous as much as 50% if pile-up phenomenon occurs during the indentation [9]. Such

This work was supported by Hannam University.
*Corresponding Author : Moon Shik Park (Hannam University)
Tel: +82-42-629-8278 email: ms.park@hannam.kr
Received August 16, 2016 Revised September 19, 2016
Accepted December 8, 2016 Published December 31, 2016

inaccuracy is due to the calculation of the actual contact area from the depth data because the underlying theories of the testing method are based on sink-in contact elasticity. Therefore, an improved method to correct this error is required especially for relatively soft materials.

In this work, a supplemental method to evaluate more accurate hardness value for pile-up situation is suggested. The proposed technique will be verified by indentation tests and finite element analyses on Al 6061 T6 and C 12200. Tensile tests were carried out to obtain the elastic and plastic responses of the materials which are given as input for the analysis. A Nano Indenter XP was used for the indentation test and the original test data were obtained. An electron microscope and other apparatus are used to observe the surface characteristics of the specimens. Finite element modeling and analysis of the Berkovich indenter and the specimen is included. Both the experiments and the analyses are discussed and conclusions are drawn.

2. Test

2.1 Tensile tests

Tensile tests were performed to obtain elastic modulus and stress-strain curves which are given as input for the finite element analysis. Specimens were sheet form 13B per KS B 0801 of aluminum Al 6061 T6 and copper C 12200. Typical soft engineering metals were selected because they may show pile-up phenomena during indentation. Details regarding the indentation tests are described in the next section. A tensile test machine (AG-10TG, Shimadzu) with an extensometer (SG50-50, Shi-madzu) was used in this work. The test results obtained at room temperature are plotted in Fig. 1.

Elastic modulus derived from the tensile test data in Fig. 1 are listed in Table 1. Elastic modulus of 75 GPa for Al 6061 T6 and 115 GPa for C 12200 were obtained. Poisson's ratios are taken from material specification per UNS C12200 or ASTM B152. The plastic part of the stress-strain curves in Fig. 1 exhibits linear hardening in the case of the aluminum sample and linear softening in the case of the copper specimen prior to the post-necking behavior. Strain softening by the copper sample shows is in agreement with the published findings [10]. Therefore, the plastic stress-strain relations are modeled with the Ludwick equation:

$$\sigma = \sigma_0 + E_p \varepsilon_p \tag{1}$$

where, σ, σ_0, E_p and ε_p are the yield stress, initial yield stress, work hardening modulus, and plastic strain, respectively. The initial yield stresses and work hardening modulus are listed in Table 1. The work hardening modulus are found to be 867 MPa and -122 MPa for Al 6061 T6 and C 12200, respectively.

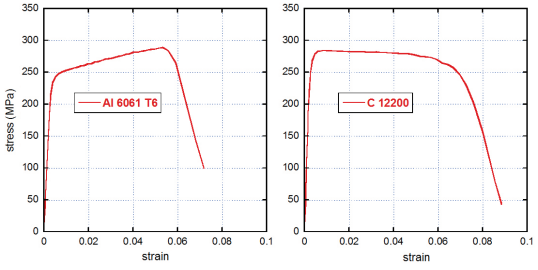

Fig. 1. Stress-strain curves of Al 6061 T6 and C 12200 obtained by tensile tests.

Table 1. Mechanical properties of the materials, as obtained by the tensile tests.

	Al 6061 T6	C 12200
Elastic modulus (GPa)	75	115
Poisson's ratio	0.33	0.34
Initial yield stress (MPa)	249	285
Work hardening modulus (MPa)	867	-122
E/σ_0, E_p/σ_0	300, 3.5	400, -0.43

2.2 Nano indentation tests

Indentation tests were performed to obtain elastic modulus and hardness values. Specimens were

10x10x5 mm rectangular blocks with the same batch as the tensile test samples. Indentation surfaces were polished to a roughness of R_a = 0.36 μm for the aluminum and, R_a = 0.23 μm for the copper. The roughness was estimated with a roughness measuring instrument (SJ-400, Mitutoyo). Indentations were carried out up to depth of 3000 nm with a nano indentation machine (Nano Indenter XP, MTS). The indentation test results are summarized in Table 2.

There are two different values for elastic modulus and hardness in Table 2; one is denoted as 'CSM averaged' while the other is termed 'from unloading' [8]. The 'CSM averaged' values are averaged from continuous stiffness measurements along with depth range of 2000~2500 nm. The 'from unloading' values are load-depth measurements obtained from the unloading after maximum indentation.

Both values of elastic modulus for the aluminum specimen were found to be 85~86 GPa, which is about 15% higher than that derived from the tensile test. The values of elastic modulus for the copper sample were 138~145 GPa, which are 20~26% higher than that obtained from the tensile test. The discrepancies in the elastic modulus measured from the tensile and the nano indentation tests are typical for soft materials because the indentation tests are erroneous if the material piles up during indentation. Hardness of 1.2~1.27 GPa for the aluminum sample and 1.3~1.4 GPa for the copper specimen were obtained. By the same reason, such hardness values seem to be erroneous for severely pile-up materials [9].

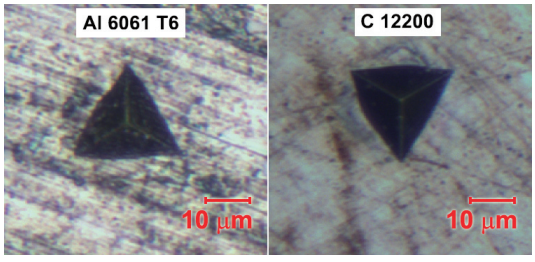

Fig. 2. Electron microscopy images of the indentation impressions on the Al 6061 T6 and C 12200 specimens.

Table 2. Mechanical properties of the materials, as obtained by the indentation tests.

	Al 6061 T6	C 12200
Elastic modulus (GPa) from unloading	86.0 (+15%)	138.1 (+20%)
Hardness from unloading	1.20	1.30
Elastic modulus (GPa) CSM averaged[§]	84.9 (+13%)	145.1 (+26%)
Hardness CSM averaged[§]	1.27	1.40

[§] Averaged over a range of 2000~2500 nm.

To see if pile-ups occur during the indentations, an electron microscope (MS-512-T, Seiwa Optical) was used to capture images of the indentation impressions; the results are shown in Fig. 2. The images that indicate outward bowing of the original triangular shapes from the top view clearly reveal the presence of pile-ups in both materials. The copper specimen exhibits more pile-ups than the aluminum. From the approximate image measurements, the maximum outward horizontal bowing displacements are 0.6 μm and 1.5 μm for the aluminum and copper samples, respectively.

The Nano Indenter XP measures the load (P) and harmonic contact stiffness (S) as the indentation process proceeds. Such measurements for the specimens are shown in Fig. 3, where h is the indentation depth in nano meters. The contact stiffness is calculated with the following equation from the theory of elastic contact [9]

$$S = 2\beta E^* \sqrt{A_c/\pi} \tag{2}$$

where E^* is the reduced modulus, β is the geometric factor for the indenter tip , and A_c is the fitted contact area:

$$1/E^* = (1-\nu^2)/E + (1-\nu_i^2)/E_i \tag{3}$$

$$A_c = C_0 h_c^2 + C_1 h_c + C_2 h_c^{0.5} \tag{4}$$

In Eq. (3), E_i and ν_i are elastic modulus and Poisson's ratio of the indenter. For a diamond indenter, the values of elastic modulus and Poisson's ratio are 1147 GPa and 0.07, respectively. Eq. (4) relates the depth of contact, h_c, to the projected area of contact, and A_c is given by the indenting machine. The theoretical projected area of contact is derived from the geometric relationships of an ideal triangular pyramid, i.e., the following cross sectional area - depth relationship:

$$A_t = 24.56h^2 \tag{5}$$

For the actual machine-specimen setup, Eq. (4) must be used instead of Eq. (5). In Eq. (4), h_c is the depth of contact for the sink-in situation [9]:

$$h_c = h - h_s \tag{6}$$

$$h_s = \varepsilon(P/S) \tag{7}$$

where, the sink-in depth, h_s, is calculated using $\varepsilon = 0.75$ for most materials when Berkovich indenter is employed [9]. In Eq. (4), the coefficients were set as $C_0 = 24.15$, $C_1 = 222.75$, and $C_2 = -1007.85$ by the Nano Indenter XP. In Eq. (2), β is the geometric factor for the indenter tip; for the Berkovich tip, 1.07 is used [9]. Therefore, the elastic modulus and hardness of the specimen are defined as:

$$E = \frac{(1-\nu^2)E_i}{2\beta\sqrt{A_c/\pi}(E_i/S) - (1-\nu_i^2)} \tag{8}$$

$$H = P/A_c \tag{9}$$

Using Eqs. (4)~(9) with basic measurements of the load (P) and contact stiffness (S) in Fig. 3, the elastic modulus (E) and hardness (H) can be calculated as in Table 2 ('CSM averaged') and Fig. 4. However, the 'from unloading' values in Table 2 are derived separately. The unloading curves in Fig. 3(a) are fitted by the following equation:

$$P_u = C(h - h_f)^m \tag{10}$$

where, C, h_f, and m are the coefficients of fitting. The contact stiffness can be calculated by differentiating Eq. (10) at the beginning of unloading as follows:

$$S_{\max} = (dP_u/dh)\big|_{h=h_{\max}} \tag{11}$$

where, $h_{\max}$ is the maximum indentation depth. The relation $S = S_{\max}$ is then used in Eqs. (7) and (8) such that the elastic modulus and hardness from unloading can be obtained as in Table 2.

Both the 'CSM averaged' and 'from unloading' measurements heavily rely on the fitted contact area from Eq. (4). However, the depth of contact, h_c, in Eq. (6) is valid only for sink-in situation. Therefore, Eq. (4) underestimates the contact area for a pile-up situation (such as in Fig. 2) and thus, Eq. (8) and (9) overestimate the modulus and hardness, as shown in Table 2. Overestimation of the elastic modulus by 13~26% is observed in Table 2. Therefore, a supplemental technique for correcting measurements of the modulus and hardness for pile-up materials is required. Such a method will be discussed in Section 4.

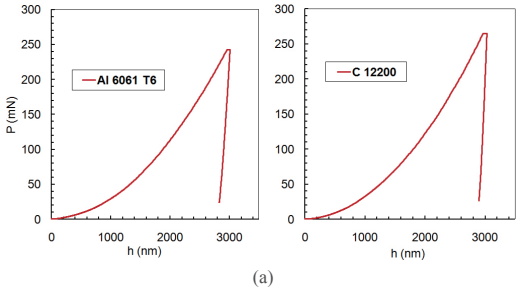

(a)

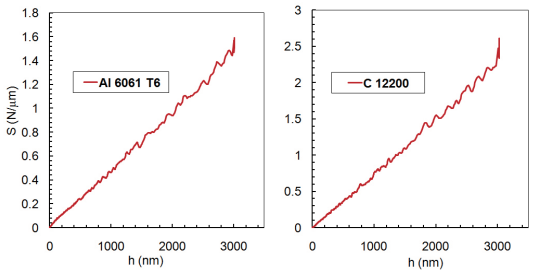

(b)

Fig. 3. (a) Load-depth curves and (b) contact stiffness-depth curves obtained from the nano indentation tests measured with Nano Indenter XP, MTS.

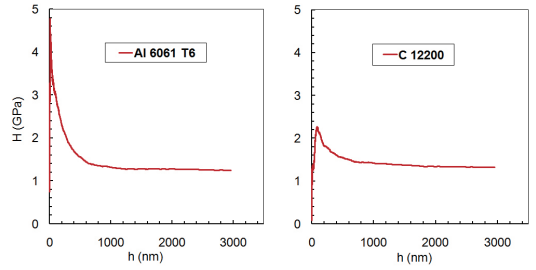

Fig. 4. Hardness-depth curves obtained from the nano indentation tests measured with Nano Indenter XP, MTS.

3. Finite Element Analysis

3.1 Three-dimensional modeling

To capture the pile-up phenomena by the indentation, finite element method is adopted here. Because of the triangular geometry of the Berkovich indenter, three-dimensional modeling is necessary to simulate indentation. An idealized triangular pyramid with a sharp tip is shown in Fig. 5 along with its angular and linear dimensions; b and c are the lengths of the edge and face with respect to the depth of indentation, h, respectively. The area of the face, depicted as the shaded area in Fig. 5, can be derived from Eq. (5) as follows:

$$A_b = (3/4)c^2 \tan\theta = \sqrt{3}\tan\theta \cdot A_t = 27.04h^2 \qquad (12)$$

Values from Eq. (12) will be compared with the contact area from the finite element analysis. The face of the indenter is modeled as a rigid surface. All edges and corners of the indenter are modeled as ideally sharp.

To reduce the modeling and computational effort, only a part of the specimen is modeled by considering the repetitive symmetry in the circular direction (in the top view). One-sixth of 360° is devised as shown in Fig. 6. Boundary conditions are applied by transforming the degrees of freedom by -30° and +30°. A relatively coarse finite element mesh is shown in Fig. 7; R is 50 μm in Fig. 6 and the height of the model in Fig. 7 is 40 μm. Abaqus is used with 13,485 linear elements for the analysis, mostly of which are hexahedron (C3D8R), and a few wedge (C3D6) elements are adopted at the center of the specimen model.

3.2 Analysis results

The indentation analysis is conducted up to an indenter displacement of 3,000 nm, from which the indenter is released to an unloaded condition. The pile-up configuration after unloading is shown in Fig. 8; the equivalent plastic strain is also displayed. The vertical pile-up (upward) displacements are 0.3 and 1.4 μm for the aluminum and copper specimens, respectively. The indentation force and contact surface area (CAREA) can be obtained for each displacement. Multiplying the calculated force and contact area by six yields the actual force and contact surface area because the model was a sixth of the full specimen. The contact surface area can be equated with Eq. (12) so that the projected contact area by the analysis is obtained as:

$$A_p = 0.91A_b \qquad (13)$$

At this point, Eq. (13) is used in Eq. (9) in place of A_c to obtain the calculated hardness values. This hardness values calculated from finite element analyses are drawn in Fig. 9(a) as dotted lines. These values are

much lower than those obtained from the original experiments in Fig 4. The reason for the discrepancy between the experimental and the analytic results will be explained in the next section.

4. Enhanced measurement of hardness

4.1 Correcting the contact area and hardness

When Eqs. (2) and (9) are combined, the following expressions are obtained.

$$H = \frac{4\beta^2}{\pi}\left(\frac{E^*}{S}\right)^2 P \tag{14}$$

$$A_c = \frac{\pi}{4}\left(\frac{S}{\beta E^*}\right)^2 \tag{15}$$

where, P and S were measured as in Fig. 3 and E^* is known from Eq. (3) using known elastic modulus values. The hardness can be obtained from Eq. (14) and thus, the use of an erroneous fitted contact area from Eq. (4) or (5) can be avoided. Instead, a new contact area A_c can be derived from Eq. (15). Meanwhile the contact stiffness S can be represented as a linear equation by fitting the data shown in Fig. 3 so that a smoother hardness can be obtained.

The hardness obtained with Eq. (14) is plotted in Fig. 9(a) with the original test data and the finite element analysis results. The hardness from Eq. (14) is quite lower than that from the original experiments but is still higher than the hardness estimated from the finite element analysis.

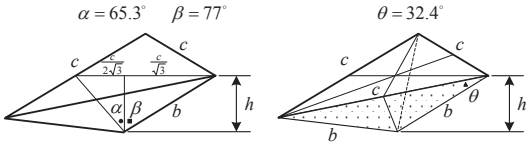

Fig. 5. Idealized Berkovich indenter geometry.

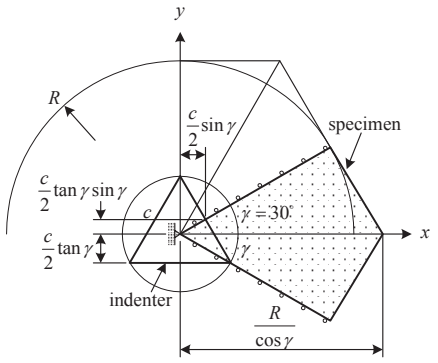

Fig. 6. 60° model and boundary conditions for the finite element analysis (top view).

The hardness values from the proposed method and the finite element method are summarized in Table 3. The reason for such different hardness values can be explained by an examination of Fig. 9(b), where ϕ is the ratio of the contact area as following, which is indicative of whether the result is pile-up or sink-in.

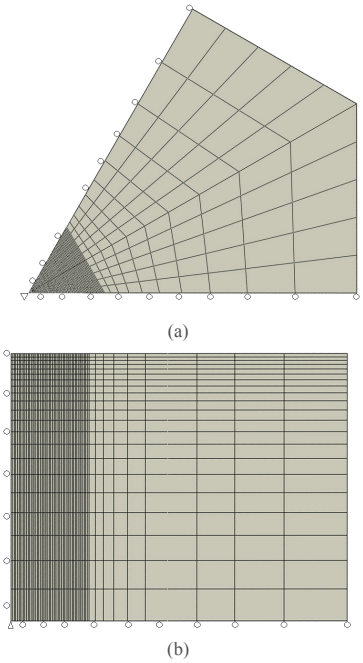

Fig. 7. Finite element mesh for the indentation specimen. (a) top view (b) front view

$$\phi = A_c / A_t \tag{16}$$

When the original measurement method is employed, the value of ϕ is less than 1.0 (sink-in) throughout the entire indentation. However, ϕ is larger than 1.0 (pile-up) by the finite element method for an indentation larger than 500 nm. When the proposed method is used, the value of ϕ lies closer to that by the finite element method, especially for aluminum. It has already been mentioned that the original measurement method significantly underestimates the contact area (as indicated in Table 2). The proposed method corrects such an underestimation when pile-up occurs. Pile-up phenomena have already been shown by the finite element method and by impression images captured with an electron microscope. However, the finite element technique tends to overestimate the contact area. This is due to the presence of size effects during the indentation. Results taking account into indentation size effects are obtained from separate works by the author [15]and are drawn as 'strain gradient plasticity' in Fig. 9(a). Such effects will be discussed in the next section.

4.2 Discussion

The proposed method gives more accurate hardness values because there is no need to use the fitted contact area in Eq. (4), which is not valid for a pile-up situation induced by the indentation. Such an improved accuracy is due to the fact that the value of P/S^2 is independent of the indentation depth or contact area [11], while the contact stiffness has a linear relationship with the contact depth according to the elastic contact theory. With the present finite element method, significant pile-ups in the Al 6061 T6 aluminum and C 12200 copper specimens are observed. For the copper sample, however, the experimental results significantly underestimate the contact area, while the finite element method significantly overestimates the contact area.

The finite element method used in this work is based on classical J_2 plasticity. However, the indentation tests reveal the existence of size effects during the indentation. These size effects increase both the strength of the material as well as the hardness due to the presence of geometrically necessary dislocations [12-14]. The density of dislocations can be related to the gradient of the plastic strain in a continuum manner. Thus, the material may respond as a strengthened material due to the indentation, especially in the nano and micro range where the indentation depths are less than 1000 nm. Hardening is clearly evident from the experiments (Fig. 4). In conclusion, a finite element method that includes dislocation-based or strain gradient-based plasticity is required to estimate indentations more accurately (partial results are shown in Fig. 9(a) as 'strain gradient plasticity').

Table 3. Hardness obtained with the proposed measurement method and finite element method.

	Al 6061 T6	C 12200
Hardness (GPa) Proposed method[§]	1.08	1.02
Hardness (GPa) Finite element method[§]	1.00	0.63

[§] Averaged over a range of 2000~2500 nm.

5. Conclusions

Al 6061 T6 and C 12200 were selected and tested as typical soft engineering metals that exhibit pile-up phenomena during indentation. The elastic and plastic responses of the materials were determined by tensile tests. The aluminum was represented as a strain hardening material, while the copper was represented as a strain softening material. Both materials were indented with a nano indentation machine. Indentation experiments were carried out up to depths of 3000 nm, which can appropriately represent the nano, micro, and macro hardness.

By the indentation tests, elastic modulus and hardness were measured. Elastic modulus was compared with those obtained from the tensile tests. The indentation tests overestimated the elastic modulus by 13~26 %. This error was confirmed due to the

evaluation of the contact area in Eq. (4) by the original measurement. Electron microscopy images clearly showed that the contacts for both materials were piled-up and thus, the areas need to be corrected.

Finite element modeling of the Berkovich indenter and specimen with the classical plasticity theory was suggested so as to minimize the modeling effort and calculation time due to the reduced total degrees of freedom by the model. The elastic and plastic data obtained from tensile tests were used in the finite element analysis. The finite element results revealed a severe pile-up phenomenon, especially for the copper specimen. It was concluded that the contact area from the indentation machine was so underestimated that the modulus and hardness were overestimated by as much as 26%.

To improve the results from the indentation experiments, a supplemental correction method for calculating the hardness that is independent of the contact depth and area was proposed. The hardness values obtained with the proposed method were 1.08 and 1.02 GPa for the aluminum and the copper specimens, respectively. These values are are 11~27% lower than those attained with the original method. The contact area estimated with the proposed method was proven to be corrected for the pile-up area. Meanwhile such contact area was lower than that from the finite element analysis.

The finite element method used in this work was based on the classical plasticity, which cannot adequately account for size effects or the dislocation density when nano and micro indentation tests are performed. Thus, dislocation-based or strain gradient-based plasticity theory is required to calculate the hardness accurately. It is known that the contact area should be smaller and the hardness should be higher if strain gradient plasticity is present. By the strain gradient plasticity which is a separate study, as mentioned in the discussion section, the analytical results are closer to those obtained with the corrected estimation of experiment proposed in this work.

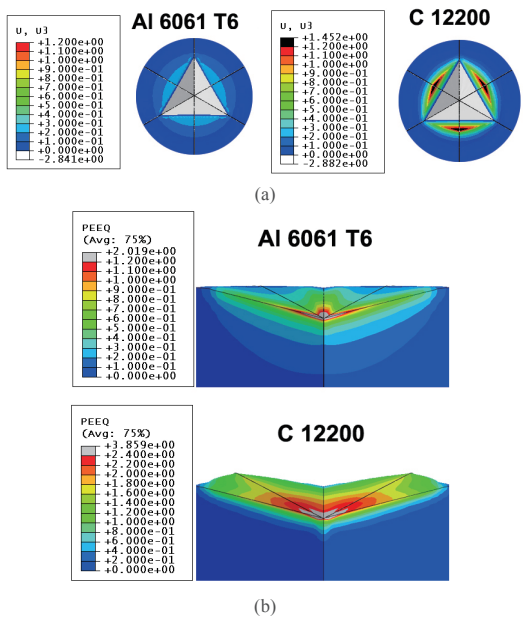

Fig. 8. (a) Vertical pile-up displacement (U3 in mm) plot and (b) equivalent plastic strain (PEEQ) plot.

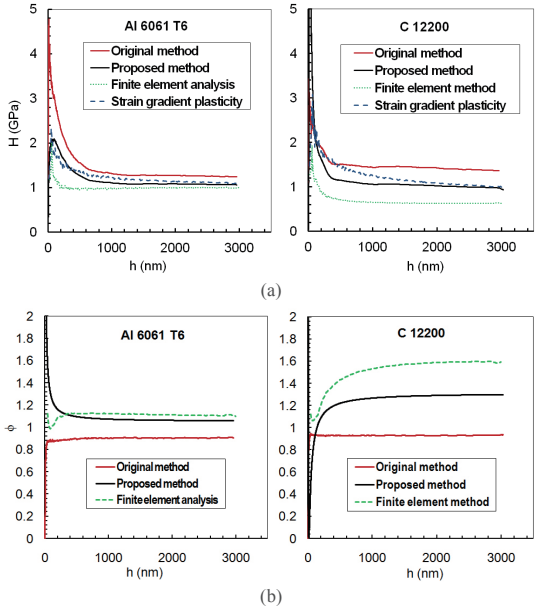

Fig. 9. (a) Hardness-depth and (b) contact area ratio-depth curves obtained with the proposed measurement method and finite element analysis method. Hardness predicted by the strain gradient plasticity is shown for reference.

References

[1] J. M. Lee, K. S. Lee, D. C. Ko and B. M. Kim, "Identification of the bulk behavior of coatings by nano indentation test and FE simulation and its application to forming analysis of the coated steel sheet," Transactions of the Korean Society of Mechanical Engineers A, 30(11), pp. 1425-1432, 2006.
DOI: http://dx.doi.org/10.3795/KSME-A.2006.30.11.1425

[2] H. Lee and J. H. Lee, "Evaluation of material characteristics by micro/nano indentation tests," Transactions of the Korean Society of Mechanical Engineers A, 32(10), pp. 805-816, 2008.
DOI: http://dx.doi.org/10.3795/KSME-A.2008.32.10.805

[3] C. H. Hong, M. Kim, J. H. Lee and H. Lee, "A conical indentation technique based on FEA solutions for property evaluation," Transactions of the Korean Society of Mechanical Engineers A, 33(9), pp. 859-869, 2009.
DOI: http://dx.doi.org/10.3795/KSME-A.2009.33.9.859

[4] B. M. Kim, C. J. Lee and J. M. Lee, "Estimations of work hardening exponents of engineering metals using residual indentation profiles of nano-indentation," Journal of Mechanical Science and Technology, 24, pp. 73~76, 2010.
DOI: http://dx.doi.org/10.1007/s12206-009-1115-8

[5] Q. Ma and D. R. Clarke, "Size dependent hardness of silver single crystals." Journal of Materials Research, 10(4), pp. 853-863, 1995.
DOI: http://dx.doi.org/10.1557/JMR.1995.0853

[6] W. J. Poole, M. F. Ashby and A. A. Fleck, Micro-hardness of annealed and work-hardened copper polycrystals, Scripta Materialia 34(4) (1996) 559-564.
DOI: http://dx.doi.org/10.1016/1359-6462(95)00524-2

[7] K. W. McElhaney, J. J. Vlassak and W. D. Nix, "Determination of indenter tip geometry and indentation contact area for depth-sensing indentation experiments." Journal of Materials Research, 13 pp. 1300-1306, 1998.
DOI: http://dx.doi.org/10.1557/JMR.1998.0185

[8] W. C. Oliver and G. M. Pharr, "Improved technique for determining hardness and elastic modulus using load and displacement sensing indentation experiments," Journal of Materials Research, 7(6), pp. 1564-1580, 1992.
DOI: http://dx.doi.org/10.1557/JMR.1992.1564

[9] W. C. Oliver and G. M. Pharr, "Measurement of hardness and elastic modulus by instrumented indentation: Advances in understanding and refinements to methodology," Journal of Material Research, 19(1), pp. 3-20, 2004.
DOI: http://dx.doi.org/10.1557/jmr.2004.19.1.3

[10] C. Moosbrugger, Atlas of stress-strain curves, ASM international, Materials Park, OH, USA, 2002.

[11] D. Joslin and W. Oliver, "A new method for analyzing data from continuous depth-sensing microindentation tests," Journal of Materials Research, 5(01), pp. 123-126, 1990.
DOI: http://dx.doi.org/10.1557/JMR.1990.0123

[12] Y. Guo, Y. Huang, H. Gao, Z. Zhuang and K. C. Hwang, "Taylor-based nonlocal theory of plasticity: Numerical studies of the micro-indentation experiments and crack tip fields." International Journal of Solids and Structures, 38(42-43), pp. 7447-7460, 2001.
DOI: http://dx.doi.org/10.1016/S0020-7683(01)00047-6

[13] G. Z. Voyiadjis and R. Peters, "Size effects in nanoindentation: an experimental and analytical study," Acta Mechanica, 211, pp. 131-152, 2010.
DOI: http://dx.doi.org/10.1007/s00707-009-0222-z

[14] Z. Shi, X. Feng, Y. Huang, J. Xiao and K. C. Hwang, "The equivalent axisymmetric model for Berkovich indenters in power-law hardening materials," International Journal of Plasticity, 26, pp. 141-148, 2010.
DOI: http://dx.doi.org/10.1016/j.ijplas.2009.06.008

[15] M. S. Park and Y. S. Suh, "Hardness estimation for pile-up materials by strain gradient plasticity incorporating the gemetrically necessary dislocation density," Journal of Mechanical Science and Technology, 27(2), pp. 525-531, 2013.
DOI: http://dx.doi.org/10.1007/s12206-012-1243-4

Moon Shik Park [Regular member]

- Feb. 1989 : KAIST, MS
- Aug. 1994 : KAIST, PhD
- Sep. 1994 ~ Feb. 1999 : Daewoo Heavy Industries Ltd., Chief Engineer
- Mar. 1999 ~ current : Hannam Univ., Dept. of Mech. Engng, Professor

<Research Interests>
Multiscale modeling of composite materials, Strain gradient plasticity, Computational mechanics of rubber and polymer materials